

The Study of Geothermal Resources in an Abnormal Volcanic-Geothermal Area in Northern China: A Case Study in Xilinhot

Wang Junhao¹, Tian Tingshan^{1,2} and Wang Qi¹

1. China University of Geosciences in Beijing, Beijing, 100083

2. Chinese Institute of Geological Environment Monitoring, Beijing, 100081

hpuwangjunhao@163.com

Keywords: Xilinhot, Geothermal resources, Hydrogeochemistry, Geothermal conditions

ABSTRACT

Xilinhot City is a typical area of volcanic geothermal anomaly in northern China. Now, the degree of research of geothermal resources is very low, basically a blank area of geothermal research. With the social and economic development, especially for the scale development of tourism, it is urgently needed to carry out research in the development conditions of geothermal resources exploration in urban and surrounding areas. Therefore, this study has academic significance and social value.

This study consists of the following three steps. First of all, based on regional geological data collection, field reconnaissance and other means, combined to previous geophysical exploration and drilling data, we analyzed the landform, stratum lithology, fractures structure, hydrogeology and geological conditions in the study area, and basically grasped the geophysical survey. Then, by using water samples collected in the field, laboratory testing, classification of water quality and geothermal iconic components, stable isotope analyzes, etc., we analyzed the hydrogeochemical characteristics in the study area and preliminarily delineated the geothermal anomaly area. Finally, combining the geophysical and hydrogeochemical conditions, the geothermal geological conditions in the study area were comprehensively analyzed for the “heat, cover, storage, connection” four basic elements, and a preliminary evaluation on the geothermal resources was made.

The research shows that: the region has the basic conditions of geothermal resources occurrence. The heat source mainly comes from the heat released from the mantle and bedrock. The cover is the Quaternary, Tertiary, Cretaceous and partly Jurassic formations and the insulation layer is mainly the Cretaceous strata. Affected by new cathaysian tectonic system, deep fractures along the north-east, north-west and east-west direction are likely to exist in this area and form the underground hot water upwelling channels.

In addition, the thermal storage situation is preliminarily evaluated in the study as follows: there may be two different heat storage areas in the north and south sides of Xilinhot, the pore type (K) and the tectonic fracture type (Pz). (1)The pore thermal storage is distributed on the fault basin on the northern side of urban areas. There are two heat reservoirs in this area: 1. Cretaceous sandstone and sandy conglomerate layers, at a depth of less than 1600m, with porosity between 10%~20%, but the water yield is not large and the salinity is relatively high, so the exploitation conditions are general. 2. The yield of fracture-karst water in Paleozoic carbonate rocks of a buried hill underlying the cretaceous strata is better, but the buried depth is larger (more than 2000 m) and the salinity ranges from 3.5 to 13.5 g/L. This water can be used for medical mineral water. (2) The structural fissure heat reservoir is mainly distributed in bedrock fissure water area in the south of the urban area. There are granite intrusions, shallow concealed at depths of 400~500 m. The thermal storage in the form of fracture belt occurs in granite rock fractured zone that is controlled by Shangdewenduo thrust fault and Limekiln normal fault. The quality and quantity of water is good. This water has good workability.

1. INTRODUCTION

Xilinhot volcanic region is located in the eastern area of Inner Mongolia high plains which are covered with a wide range of magmatic rocks in northern China. Volcanic activity in this region possessed the characteristics of multi-stage eruptions during the period from Paleozoic to Cenozoic in the long geological evolution process, and its tectonic environment is very complex. The quality of geothermal resources in this area has close relationship with the geological structure conditions, rocks thermal conductivity, volcanic and magmatic activity, and hydrogeological factors. This study makes a comprehensive analysis of the geothermal geological conditions in the region and performs a preliminary evaluation of geothermal resources by employing integrated geophysical and geochemical methods. This study would be of great significance to fill the gaps of the study of geothermal resources in this region.

2. REGIONAL GEOLOGICAL CONDITIONS

The study area is located in the region between Hegenshan ophiolite belt and Xar Moron River Fault Zone, which has gone through a series of tectonic rifting such as subduction, collision and stretching, and eventually forms a combination of large number of magmatic rocks in different tectonic environments. The structural outline of a large area has obvious characteristics of Paleozoic geosynclinal environmental features: the structural direction of close linear folds is trending towards NE and EW; most folds in Mesozoic period are minor axis folds, trending towards NE; developed fractures are mainly trending towards NE, NW and EW. Particularly, the north-west trending faults formed later among these faults. Into the Mesozoic era, the north-east rift basins and volcanic eruption basins formed. During that period, Xilinhaote Erlian Basin region and Erlian basins were developed well. The Erlian basins are a Mesozoic rift basins group on the base of Inner Mongolia-Daxinganling Hercynian fold belt (Figure 1). The major sedimentary strata of the basins are Lower Cretaceous Bayanhua group, and the study area is at the eastern edge of the basin group uplift belt.

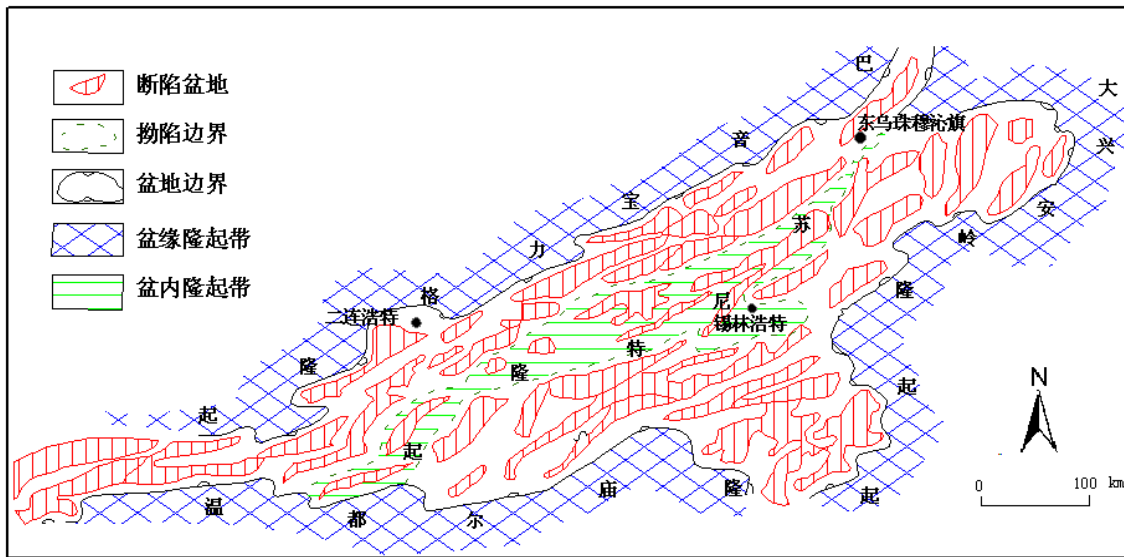
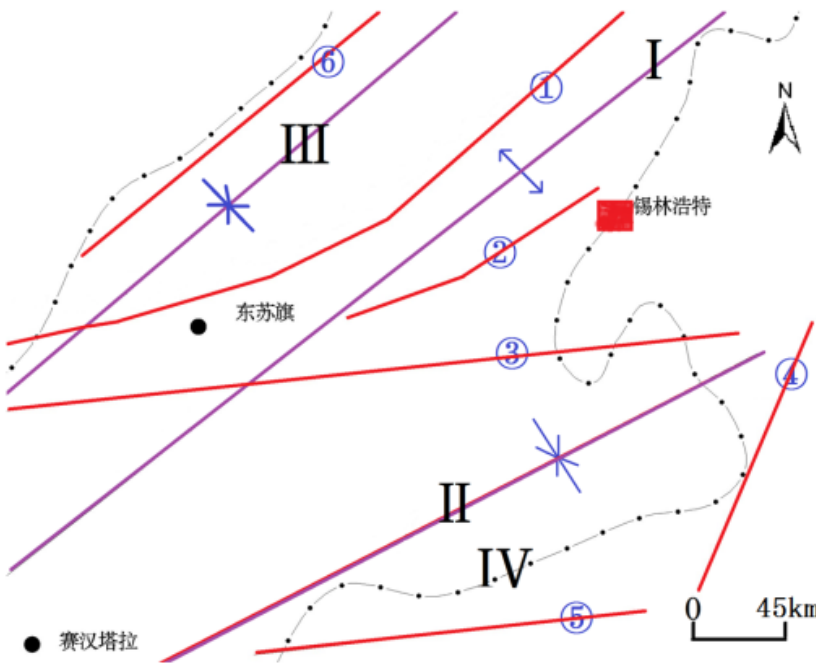


Figure 1: Erlian rift basins group tectonic units figure (according to Jianye, 1998, slightly modified)

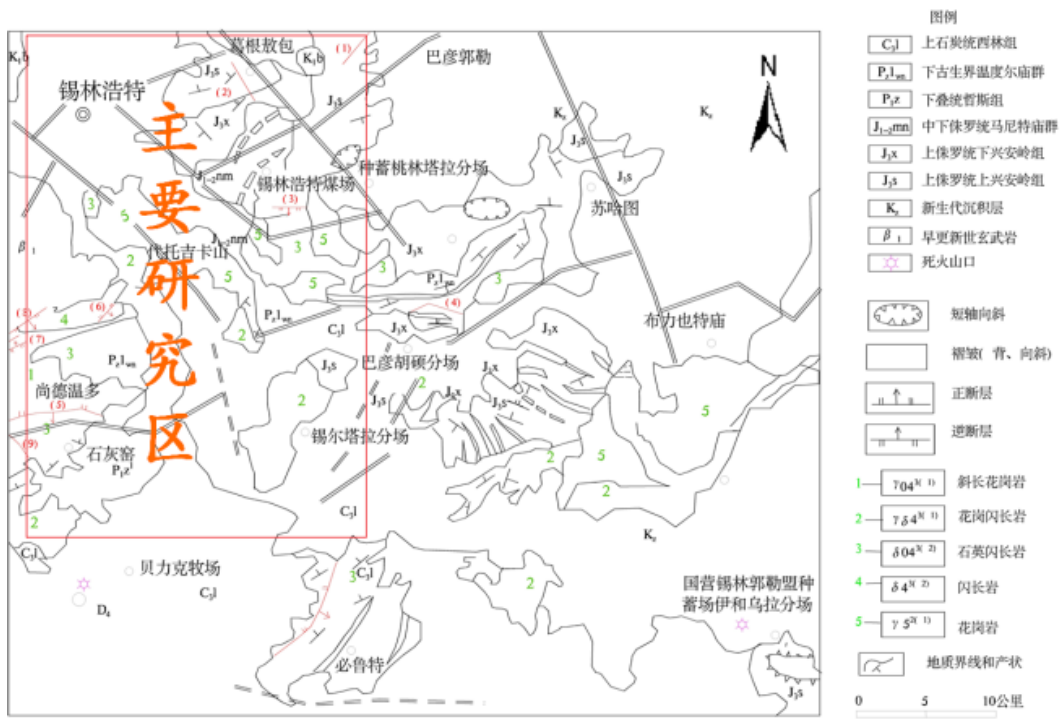
Hegenshan fracture and Xar Moron River fracture have an important impact on the study area. Among them, Hegenshan fracture is located in north-central Erlian Basin, trending towards NEE, and the tendency towards NW extends up to 750 km or more, as a super-lithospheric rupture. Xar Moron River fracture is located in south-central Erlian Basin which is a super-lithospheric rupture trending towards EW and with tendency towards north, extending up to more than 700 km. The fracture was a thrust fault in the late Paleozoic and Mesozoic, and a tensile fracture in the Cenozoic Era. Figure 2 shows the regional tectonic background of the study area. The cut depths of Hegenshan fault zones and Green Pasture fault reach 30 km and 15 km respectively, and the cut depth of Xar Moron River Fault and Lindsey fault zones is up to 40km. There is a deep fault cutting to Moho near Xar Moron River. From the view of large regional geological structure, Hegenshan fracture, Xar Moron River fracture, Lindsey fracture and Green Pasture fracture adjoining the study area have a controlling effect on the distribution structure of a small area in the study area.



注: ①贺根山断裂; ②达青牧场断裂; ③西拉木伦河断裂; ④林西断裂; ⑤腾格爾南断裂;
⑥沙那断裂; I 锡林浩特复背斜; II 赛汉塔拉复向斜; III 贺根山-索伦向斜; IV 盆地边界

Figure 2: Regional tectonic background sketch of study area

From the view of small regional geological structure, local magmatic activity is frequent, and folds and faults develop intensely in the study area because of the influence of the previous tectonic movements. Xilinhot northwestern region belongs to ridge beam uplift, and the eastern part belongs to Baiyinwula uplift. It is likely to develop pressurized fractures in the transition zone between the uplift and the middle part of the depressed zone. Therefore, Maodeng rift basin formed in the middle location, and is connected with southwest leap rift basin. Several tensional faults trending towards NW formed at the adjoining zone of the two rift basins, developing a checkerboard structure by the combination with pressurized fracture which trends towards NE (Figure 3).



注: — 与 = 分别表示根据地面电法和钻孔资料推测的隐伏断层

Figure 3: Xilinhote area tectonic outline sketch

Parallel ridges, depression zone pressure (twist) fractures and associated tensile, torsional tensional faults, all develop well in the study area, and control the formation of secondary rift basins in the northern part of the study area. During the Late Jurassic to Early Cretaceous period, a series of uplifts, depression (rift) zones, parallel pressure (twist) fractures and associated tensional (torsional) faults distributed in the bedrock hilly area before the Cretaceous, and they can be classified into four groups: NE, NEE, NNE and NW. The first three sets of fractures formed under the effect of pressure or twisted action, and most of them are filled with quartz and granite veins, so the ability of water storage of these fractures is weak or they can block water flow. NW-trending faults are tensile fractures. NW-trending valley formed at this zone with good ability of water storage.

3. HYDROGEOCHEMICAL CHARACTERISTICS

Chemical characteristics of the water body reflect a state of equilibrium between the water and the surrounding environment. The origin of the water can be explained, or the deep geothermal reservoir physical and chemical environment which it had experienced can be predicted, according to the chemical composition and type of water. Through the study of geothermal landmark components of various types of water in the study area, a geothermal anomaly range can be delineated by using the dispersion halos of these components. And then, determine underground thermal water rising migration channel, providing a scientific basis for determining the drilling location.

This exploration of geothermal resources can be carried out in two different types of places according to the geological - hydrogeological conditions (Fig. 4). The first type is a small rift basin in the northern part. Due to the thick overlying sedimentary strata, if geothermal gradient is stable, then it would be possible to find the geothermal resources needed at a certain depth under the ground. The initial forecast is that Cretaceous conglomerate layer which has rich water may be the thermal reservoir in this area; the second type is the southern part where bedrock fractures developed well. If a deep fault communicates with the deep heat source, then the bedrock fissure water would bring deep geothermal energy to the surface through deep water circulation. The main heat storage in this region is granite fractured zone at the depth of 400 m.

Researchers survey 40 points in the field, and detect and collect water samples in 37 of these points (Figure 5). In this study, bedrock fissure water in the southern part of the study area and loose rock pore water in the northern Xilinhote rift basins are sampled to achieve a reasonable coverage. It should be noted that, due to all collected water samples being within 100 m underground from shallow water or surface water, following in this article they are regarded as the same aquifer for the analysis.

Water samples are classified into types into these four kinds of water body types: motor-pumped well, springs, mineral springs, rivers and public wells (large wells), and tests and analysis are carried out in water samples. In the laboratory, Na^+ , K^+ , Ca^{2+} , Mg^{2+} , Cl^- , SO_4^{2-} , F^- , HCO_3^- , $HSiO_2^-$, CO_3^{2-} , pH values of these water samples are analyzed and detected (Schedule).

The content of components of the groundwater affected by geothermal activity is significantly different from the common groundwater. Generally, conductivity and TDS values are higher in the water body affected by geothermal fluids. This is due to the relatively strong water-rock interaction in high temperature environments, making the water salinity increase, and enhancing conductivity. The conductivity of water samples and the distribution of conductivity anomaly area are showed in Figure 6.

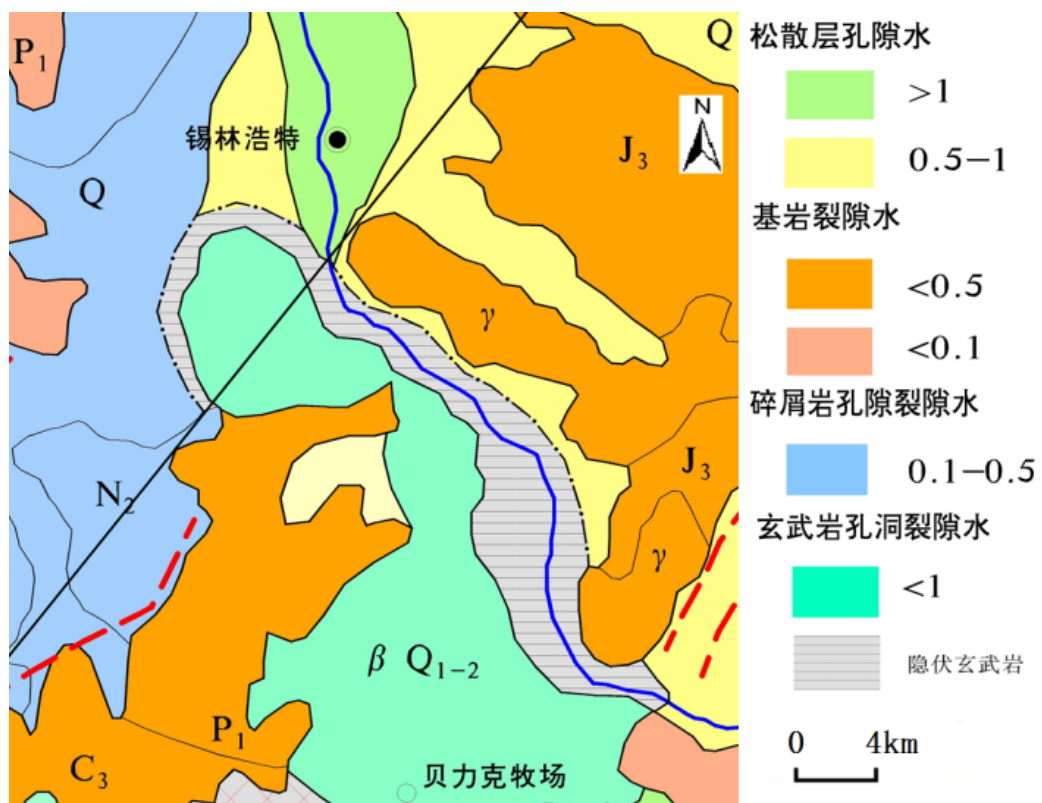


Figure 4: Hydrogeological division sketch of study area

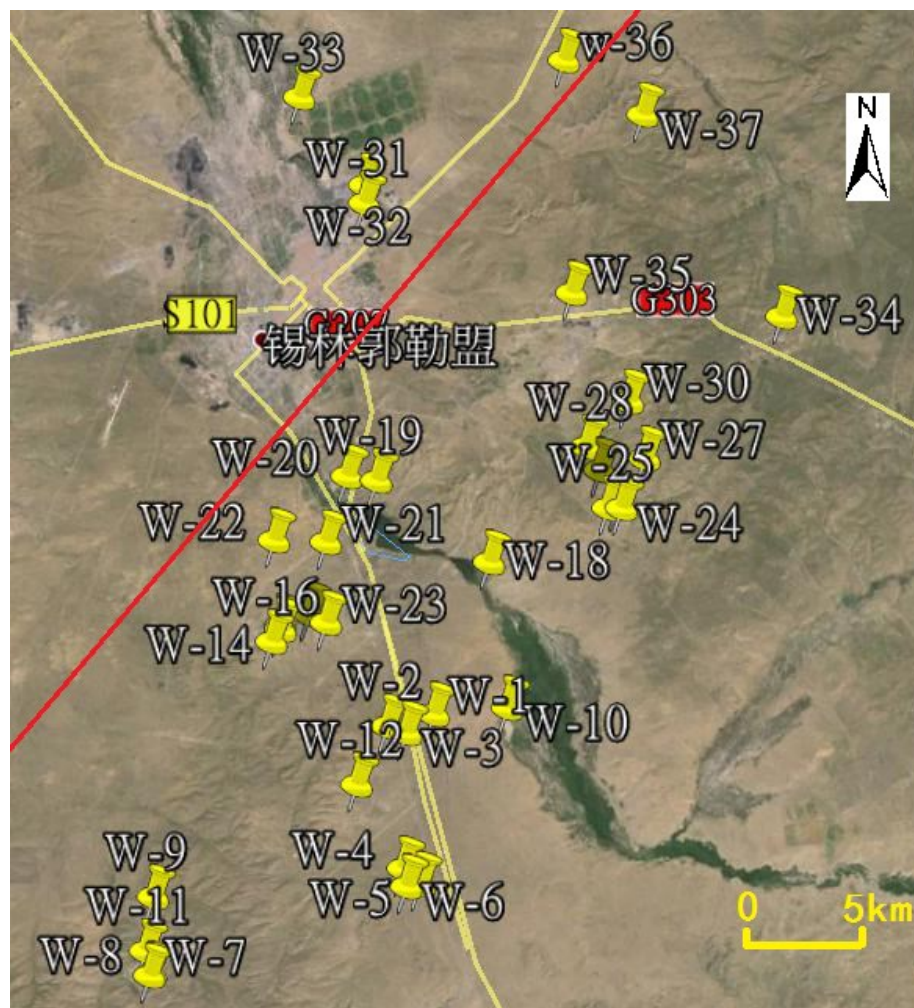


Figure 5: Remote distribution sketch of collection water points in the study area

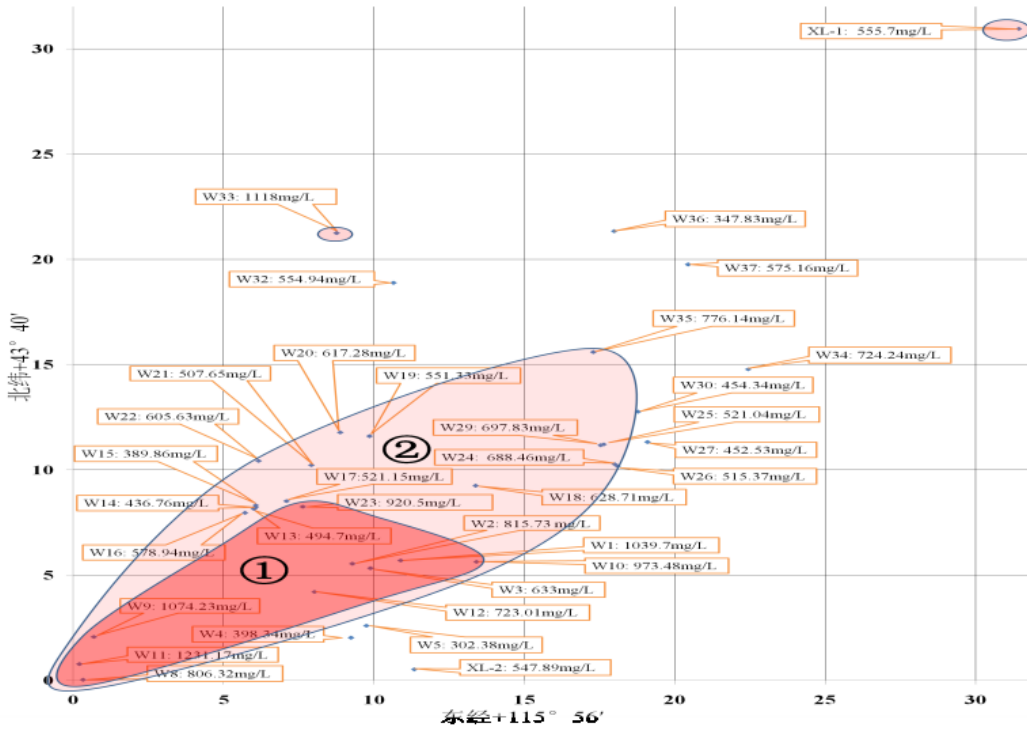


Figure 6: Distribution map of TDS values. * Note: ① TDS values greater than 800mg / L of high anomaly areas; ② the range of TDS values are 600 ~ 800mg / L of the abnormal area.

This study shows that the indicative contents of Na^+ , K^+ , Ca^{2+} , Mg^{2+} , Cl^- , SO_4^{2-} , F^- , HCO_3^- , HSiO_2^- , and CO_3^{2-} , in these water samples are high except for Ca^{2+} , Mg^{2+} , and HCO_3^- . This result indicates the water is affected by underground hot water. Water quality types available are summarized in Table 1 according to test results.

Calculate $(\text{Na}^+ + \text{K}^+)$ and $(\text{CO}_3^{2-} + \text{HCO}_3^-)$ mg equivalent percentage, and draw Lange QC - Ludwig diagram, showed in Figure 7.

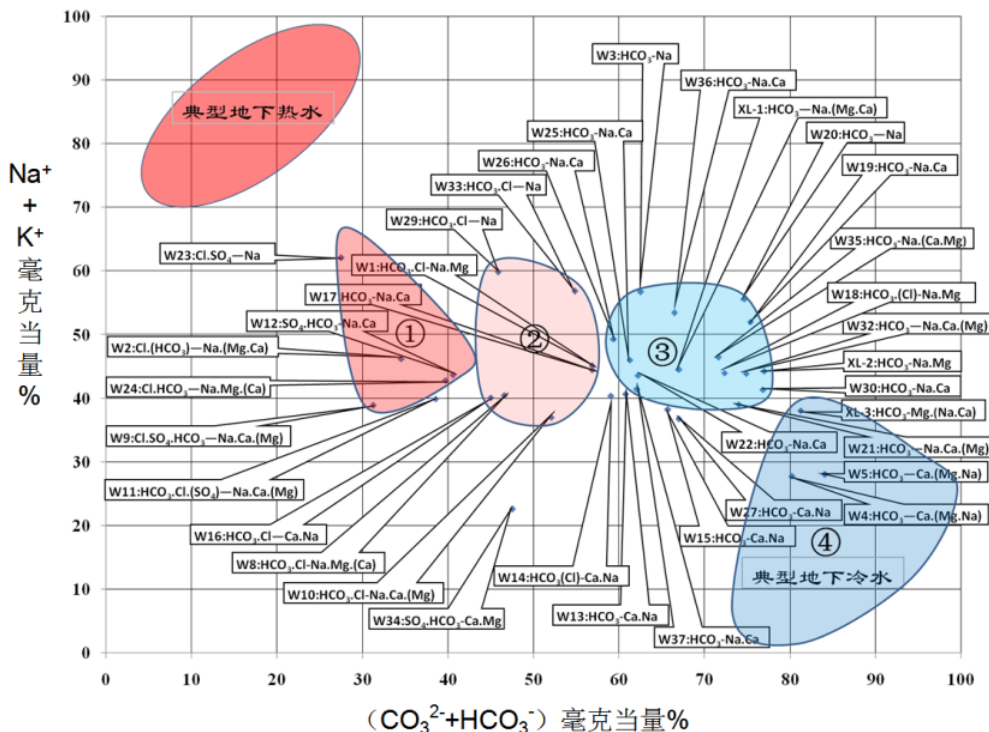


Figure 7: L-L diagram

Table 1 Water quality types of each type of water samples statistics tables

Water types	Numbers of water samples	Water quality types
Motor-pumped well	XL-1	HCO ₃ —Na.(Mg.Ca)
	W1	HCO ₃ .(Cl)—Na.Mg
	W2	Cl.(HCO ₃)—Na.(Mg.Ca)
	W3	HCO ₃ —Na
	W4	HCO ₃ —Ca.(Mg.Na)
	W5	HCO ₃ —Ca.(Mg.Na)
	W8	HCO ₃ .Cl—Na.Mg.(Ca)
	W9	SO ₄ .Cl.HCO ₃ —Na.Ca.(Mg)
	W10	HCO ₃ .Cl—Na.Ca.(Mg)
	W12	SO ₄ .HCO ₃ —Na.Ca
	W16	HCO ₃ .Cl—Ca.Na
	W17	HCO ₃ —Na.Ca
	W21	HCO ₃ —Na.Ca.(Mg)
	W22	HCO ₃ —Na.Ca
	W23	Cl.SO ₄ —Na
	W26	HCO ₃ —Na.Ca
	W27	HCO ₃ —Ca.Na
	W29	HCO ₃ .Cl—Na
	W30	HCO ₃ —Na.Ca
	W32	HCO ₃ —Na.Ca(Mg)
	W33	HCO ₃ .Cl—Na
	W35	HCO ₃ —Na.(Ca.Mg)
	W36	HCO ₃ —Na.Ca
mine water	W11	CO ₃ .Cl.(SO ₄)—Na.Ca.(Mg)
mineral springs	XL-3	HCO ₃ —Mg.(Na.Ca)
springs	W15	HCO ₃ —Ca.Na
rivers	XL-2	HCO ₃ —Na.Mg
	W18	HCO ₃ .(Cl)—Na.Mg
	W19	HCO ₃ —Na.Ca
	W20	HCO ₃ —Na
public wells	W13	HCO ₃ —Ca.Na
	W14	HCO ₃ .(Cl)—Ca.Na
	W24	Cl.HCO ₃ —Na.Mg.(Ca)
	W25	HCO ₃ —Na.Ca
	W34	SO ₄ .HCO ₃ —Ca.Mg
	W37	HCO ₃ —Na.Ca

Lange QC - Ludwig diagram (Figure 7) can clearly show the chemical characteristics of the water body which each water sample belongs to. Particularly, typical geothermal water is located in the upper left diagram where Na⁺ is the main cation and Cl⁻ or SO₄²⁻ is the main anion. The meaning of the illustration for each water sample in the survey area is as followed: Na⁺ is rich in the upper side of this diagram, and it perhaps relates to deep geothermal fluid leak. Figure 7 indicates that water samples collected in this survey could be divided into four types: 1. cations and anions are all affected by geothermal water, Na⁺ is the main cation, Cl⁻ and SO₄²⁻ are the main anions, and the secondary major anion is HCO₃⁻; 2. Type of water that transits from cold to hot water, with Na⁺ as the main cation, and HCO₃⁻ as the main anion; 3. cold type water whose cations are affected by geothermal water; 4. typical cold water type where Ca²⁺ and Mg²⁺ are the main cations, and HCO₃⁻ is the main anion. Figure 7 shows that W11 is the transitional type between 1 and 2, and W13, W14, W15, W27 all belong to HCO₃⁻—Na.Ca type of water, the transitional type between 2 and 3. In addition, despite isolated location, W34 belongs to the type of water affected by cold water and its content of Na is low. The distribution of these four types of water in this study area is shown in Figure 8 which indicates that the regularity is similar to the preceding Figure 6.

The special chemical components contained in geothermal water reach high levels, thus constitute mineral water, which is the result of the contents of these corresponding components of groundwater, accumulates through the deep underground cycle. Silicic acid and fluoride contents could be the landmark components to identify geothermal water because their content in the groundwater is usually significantly higher than their content in the underground cold water and surface water. Silicic acid and fluoride contents of all the water samples involved in this study are listed in Table 2, and their abnormal regions are shown in Figure 9 and Figure 10.

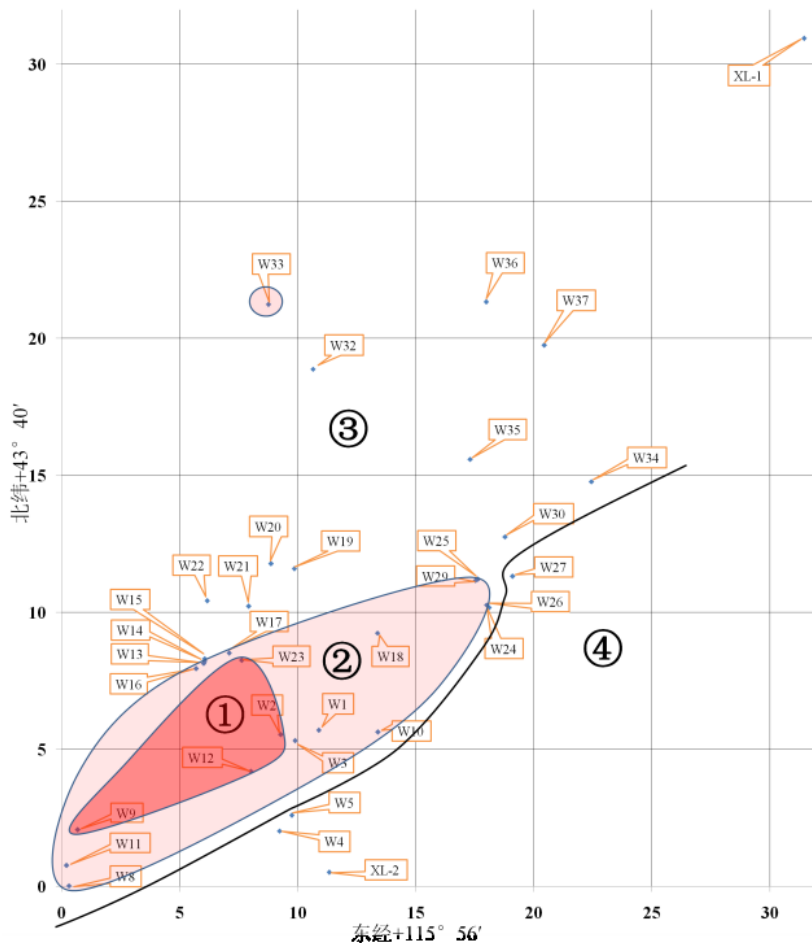


Figure 8 Water chemistry type geothermal anomaly zoning maps. * Note: 1 high abnormal area; 2 abnormal area; 3 slightly abnormal area; 4 typical cold type area.

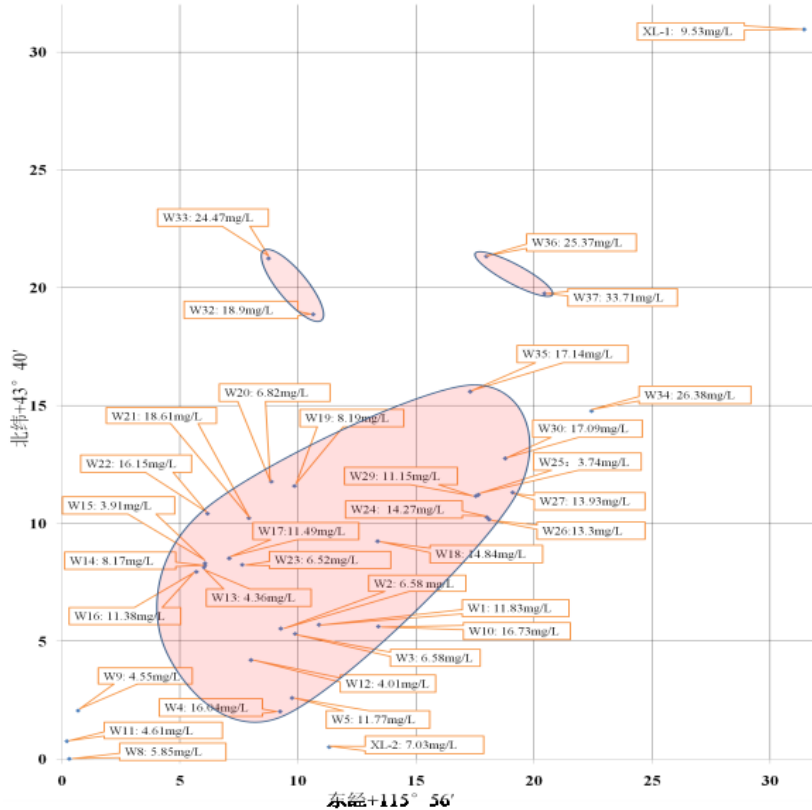


Figure 9: Distribution map of silicic acid content of each water sample. *Note: the shaded part indicates silicic acid content greater than 11mg / L which is the abnormal area.

Table 1 Water quality types of each type of water samples statistics tables

Water types	Numbers of water samples	Water quality types
Motor-pumped well	XL-1	HCO ₃ —Na.(Mg.Ca)
	W1	HCO ₃ .(Cl)—Na.Mg
	W2	Cl.(HCO ₃)—Na.(Mg.Ca)
	W3	HCO ₃ —Na
	W4	HCO ₃ —Ca.(Mg.Na)
	W5	HCO ₃ —Ca.(Mg.Na)
	W8	HCO ₃ .Cl—Na.Mg.(Ca)
	W9	SO ₄ .Cl.HCO ₃ —Na.Ca.(Mg)
	W10	HCO ₃ .Cl—Na.Ca.(Mg)
	W12	SO ₄ .HCO ₃ —Na.Ca
	W16	HCO ₃ .Cl—Ca.Na
	W17	HCO ₃ —Na.Ca
	W21	HCO ₃ —Na.Ca.(Mg)
	W22	HCO ₃ —Na.Ca
	W23	Cl.SO ₄ —Na
	W26	HCO ₃ —Na.Ca
	W27	HCO ₃ —Ca.Na
	W29	HCO ₃ .Cl—Na
	W30	HCO ₃ —Na.Ca
	W32	HCO ₃ —Na.Ca(Mg)
	W33	HCO ₃ .Cl—Na
	W35	HCO ₃ —Na.(Ca.Mg)
	W36	HCO ₃ —Na.Ca
mine water	W11	CO ₃ .Cl.(SO ₄)—Na.Ca.(Mg)
mineral springs	XL-3	HCO ₃ —Mg.(Na.Ca)
springs	W15	HCO ₃ —Ca.Na
rivers	XL-2	HCO ₃ —Na.Mg
	W18	HCO ₃ .(Cl)—Na.Mg
	W19	HCO ₃ —Na.Ca
	W20	HCO ₃ —Na
public wells	W13	HCO ₃ —Ca.Na
	W14	HCO ₃ .(Cl)—Ca.Na
	W24	Cl.HCO ₃ —Na.Mg.(Ca)
	W25	HCO ₃ —Na.Ca
	W34	SO ₄ .HCO ₃ —Ca.Mg
	W37	HCO ₃ —Na.Ca

Calculate the potassium-magnesium (K-Mg) temperature scale and quartz (SiO₂) temperature scale by using the results detected in 36 water samples collected in this field survey. The calculated results of geochemical temperature scale are shown in Table 3, and potassium-magnesium (K-Mg) temperature scale anomalous areas are delineated as shown Figure 11.

Carry out line fitting analysis by using deuterium (D), oxygen-18 (18O) data of water samples and precipitation data (Figure 12). The investment points of D and 18O measurements results of various water samples on the linear relationship between δD and $\delta^{18}\text{O}$ of global precipitation, and are not only close to the line but also concentrated (Figure 12). This indicates that the origin of groundwater in this area is precipitation despite being gathered from different sources. In addition, these water samples in the study area show significant 18O drift, which indicates, at certain scale, concealed geothermal resources underground in this area, with a considerable impact on shallow groundwater and surface water.

More consistent degree of agreement about hydrogeochemical anomalies area could be determined by analyzing and researching TDS of water samples in this region, water chemical types, geothermal landmark components, geochemistry temperature scale, stable isotopes and many other indicators. In the area, deep geothermal components outcrop in surface. The phenomenon of geothermal components anomalies and deep geological structural conditions are closely related in this region (Figure 14).

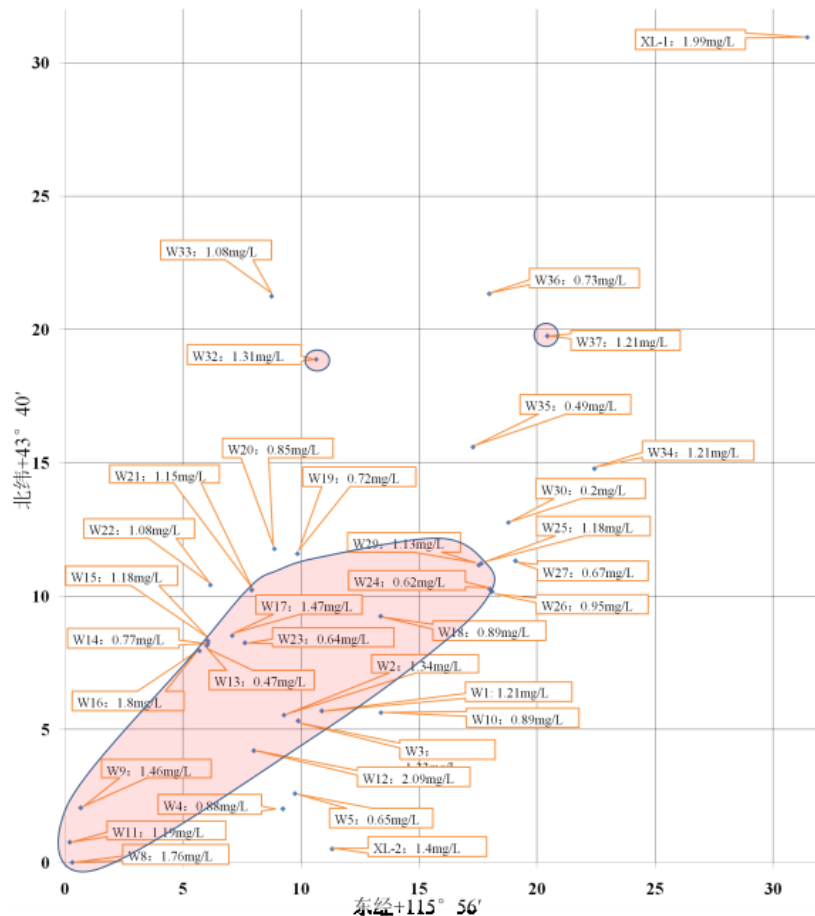


Figure 10 Content distribution map of each water sample. *Note: The shaded part indicates F content greater than 1.1mg/L which is abnormal areas.

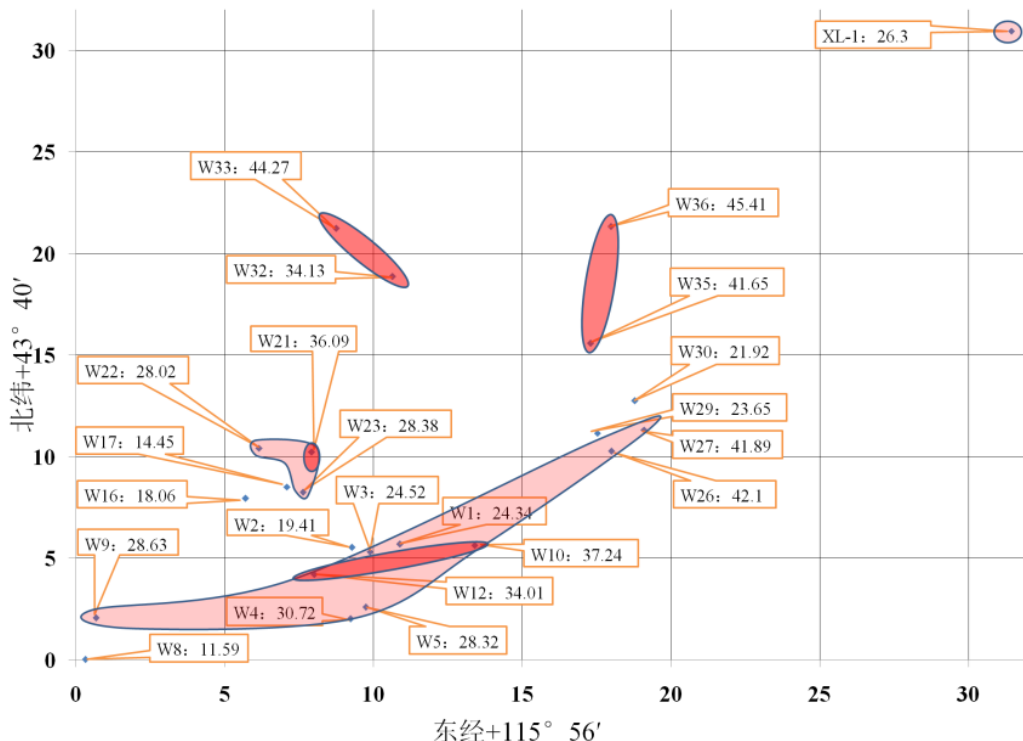


Figure 11: Distribution map of potassium and magnesium temperature scale. Note: The dark areas represent potassium and magnesium temperature scale greater than 34°C; light colored area represents potassium and magnesium temperature scale is between 24 ~ 34 °C.

Table 3 geochemical temperature scale calculations

Water types	Numbers of water samples	Quartz temperature scale - no steam loss /°C		K-Mg temperature scale /°C	
		Measured values	Mean	Measured values	Mean
Motor-pumped well	XL-1	37.71	45.012	26.3	29.79
	W1	44.8		24.34	
	W2	26.27		19.41	
	W3	26.27		24.52	
	W4	55.35		30.72	
	W5	44.63		28.32	
	W12	12.23		34.01	
	W16	43.5		18.06	
	W17	43.82		14.45	
	W8	22.81		11.59	
	W9	15.69		28.63	
	W10	56.86		37.24	
	W21	60.76		36.09	
	W22	55.59		28.02	
	W23	26		28.38	
	W26	48.78		42.1	
	W27	50.38		41.89	
	W29	42.83		23.65	
	W30	57.63		21.92	
	W32	61.33		34.13	
	W33	71.2		44.27	
	W35	58.31		41.65	
	W36	72.63		45.41	
mine water	W11	16.05	16.05	32.08	32.08
mineral	XL-3	61.72	61.72	23.31	23.31
springs	W15	11.55	11.55	34.03	34.03
rivers	XL-2	28.25	35.28	51.41	51.76
	W18	52.59		46.03	
	W19	32.93		56.25	
	W20	27.34		53.36	
public wells	W13	14.51	44.57	37.49	38.56
	W14	32.85		76.21	
	W24	51.22		21.22	
	W25	10.36		40.31	
	W34	74.18		18.06	
	W37	84.28		38.06	

4. COMPREHENSIVE ANALYSIS OF GEOTHERMAL GEOLOGICAL CONDITIONS

According to the analysis of the geological conditions, the study area can be divided into two areas for research, north and south (Figure 4 and Figure 5), namely the north sedimentary basin type and the southern district of bedrock fault zone. Both heat sources are derived from the heat released by the mantle and bedrock. Among them, the sedimentary basin in the north is mainly the layered porous thermal storage and the bedrock tectonic fault zone in the southern district is priority due to the banded fractural thermal storage.

4.1 Sedimentary basin

As a typical intraplate fault basin of rift valley, the northern district has significant fault activity, but there is no surface geothermal display. The temperature of the geothermal reservoir increases steadily with depth, usually at 2000 m it reaches above 70°C. Its heat source mainly comes from the normal geothermal depth, but there is also local heat convection. The main geothermal reservoir in this area is the cretaceous sandstone, its thickness is 1000~3000 m in general. The features of the three vertical formations can be summarized as "upper coarse, middle fine and lower coarse". The middle fine group is mainly mudstone, the upper coarse group and lower coarse group are mainly glutinite, which constitute the main aquifer. Among them, the upper sedimentary strata are coarse gravel strata and their watery and transmissibility is better. However, they cannot form a good thermal reservoir because of its shallow depth. Therefore, the sedimentary basin region is given priority to the layered pore geothermal reservoir in the lower part of Cretaceous Bayanhua group. The lithology of thermal reservoir strata is mainly conglomerate and glutinite. The region belongs to the temperate semi-arid continental monsoon climate zone, annual average temperature is 0~3°C. The heat flow value is between 60~70 mw/m² and the geothermal gradient is between 2~2.5°C / 100 m, which is below the average geothermal gradient. According to the existing geological data in the study area, the Cenozoic sequence in this basin is very thin, with thickness

not exceeding 200~500 m, while the largest thickness of the Quaternary, Tertiary and Cretaceous Cayanhua Group is 1900 m. The thickness of the Cretaceous sedimentary strata is about 1600 m, where the sedimentary thickness is 1400 m in the upper Cretaceous and 200 m in the lower Cretaceous.

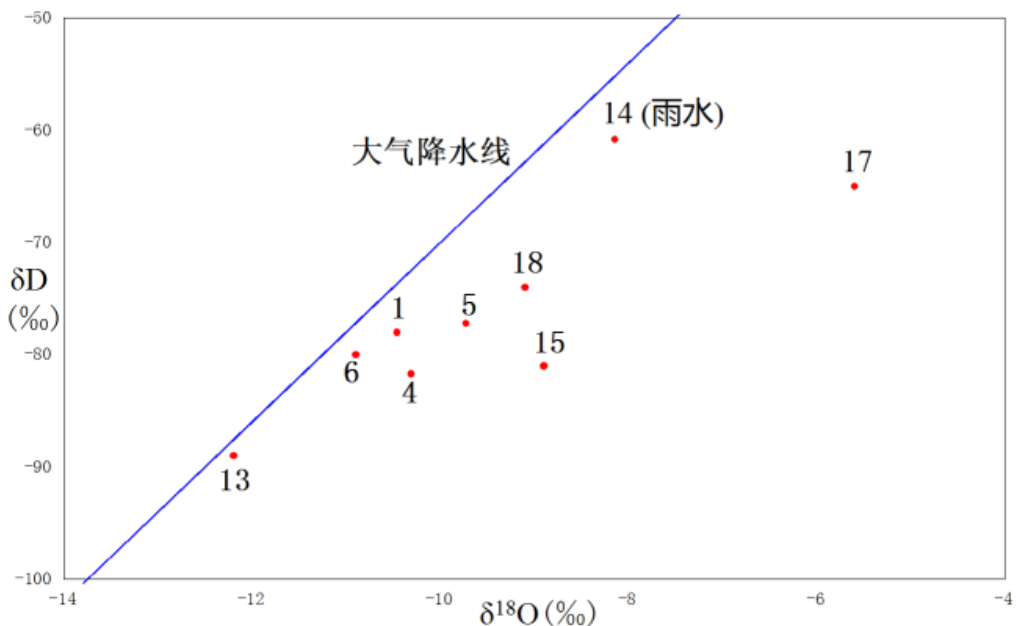


Figure 12: Relationship diagram of δD and $\delta^{18}\text{O}$ values

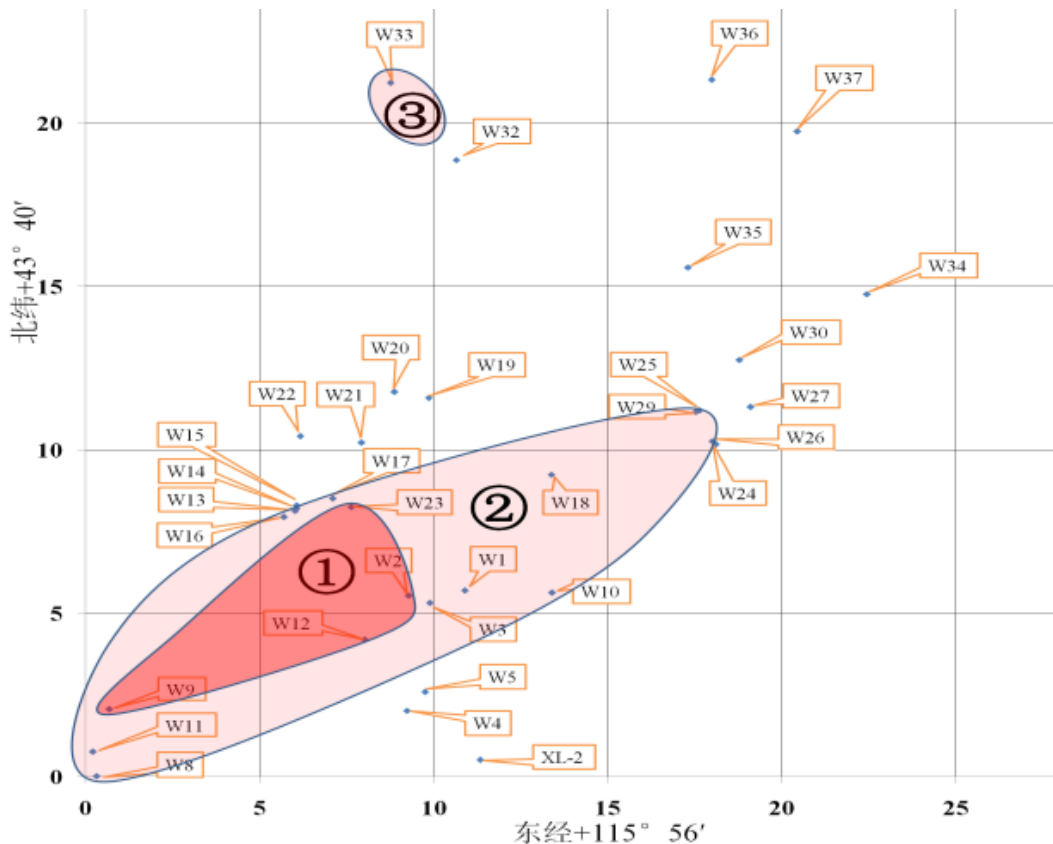


Figure 13: Distribution map of complicated geochemical anomalies degree. Note: 1 geothermal component highly unusual display area; 2 and 3 geothermal component common abnormal display area.

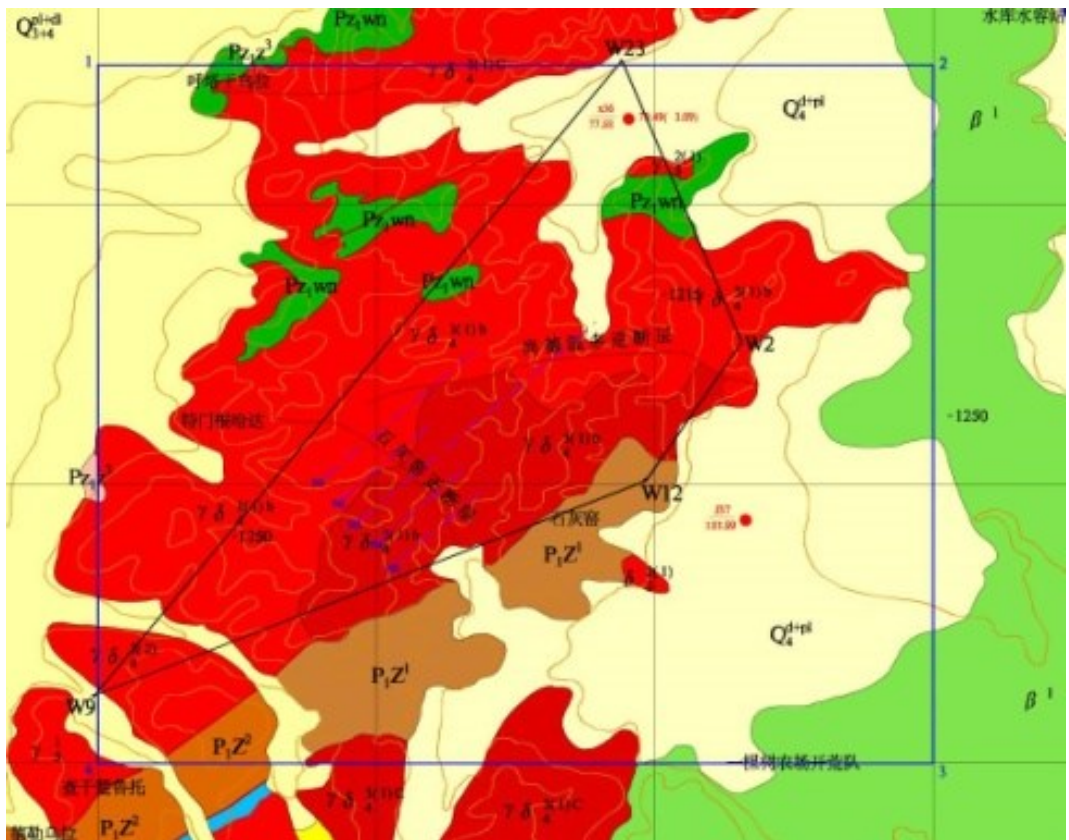


Figure 14: Fitting of water chemistry highly unusual region and geological structural condition. Note: Limekiln is positive fault and Suntech Windsor Fault is in this figure a reverse fault.

Combining the information above, in accordance with the formula for the temperature of geothermal reservoir in sedimentary basins, a preliminary calculation concludes that the temperature of geothermal water reservoir in the Upper Cretaceous is about 43~50.5°C, the temperature of the geothermal reservoir in Lower Cretaceous is about 48~55.5°C, and the temperature of the Paleozoic carbonate fractured karst reservoir in the buried hill underlying the Cretaceous strata is up to more than 63°C.

According to the calculation of geochemical geothermometer for geothermal standard components of three water samples (W33, W35 and W36) collected within this region, we can know: the heat reservoir temperatures calculated by potassium and magnesium geothermometers are 44.27°C, 41.65°C and 45.41°C, respectively; and the calculated heat reservoir temperatures using quartz geothermometer are 71.2°C, 58.31°C and 72.63°C, respectively. Thus, the conservative values of thermal reservoir temperature calculated using two ways of geothermal gradient and geothermal geothermometer is consistent, both are about 45°C. Affected by the factors of geothermal gradients in different depths, the maximum of thermal storage may also be up to the thermal storage temperature indicated by quartz geothermometer, namely it can reach 70°C. According to the oil drilling data obtained from the graben basin in North District, this conclusion has been well verified.

4.2 Bedrock fault zone

Controlled by tectonic movement and affected by a multi-stage, multi-directional tectonic stress field, there is a certain scale of fracture belt and deep fault belt between the sedimentary basin and the tectonic uplift area. The underground circulating hot water of the granite fractured zone in southern district constitutes a bedrock fractured structural geothermal reservoir, always present zonal or vein. Its development rules and distribution characteristics are controlled by the conditions of fault structure and have obvious anisotropy. The type of surrounding rock for thermal storage are mainly the early Yanshan granite, the later Variscan granite and granodiorite, characterized by heat storage in belt and vein fissure. The underground water is mostly in the form of confined water.

Using the ratio relationships of potassium and magnesium content in the water samples collected, the temperature of the recoverable heat storage at less depth can be calculated using the potassium-magnesium temperature geothermometer formula. The potassium and magnesium geothermometers show that the temperature of this area is up to 34~42°C (W10, 12, 21, 26, 27).

Using silica content in groundwater and according to a quartz geothermometer formula, the temperature of the deep underground heat reservoir can be calculated. The quartz geothermometer shows that the temperature of regional heat reservoir can reach 55~60°C (W4, 10, 21, 22, 26, 27, 30).

4.3 Geothermal model and prediction of circulation depth

The conceptual models of the graben basin in the northern part of the study area and the bedrock structural fissure zone in the southern part can be expressed as in Figure 15.

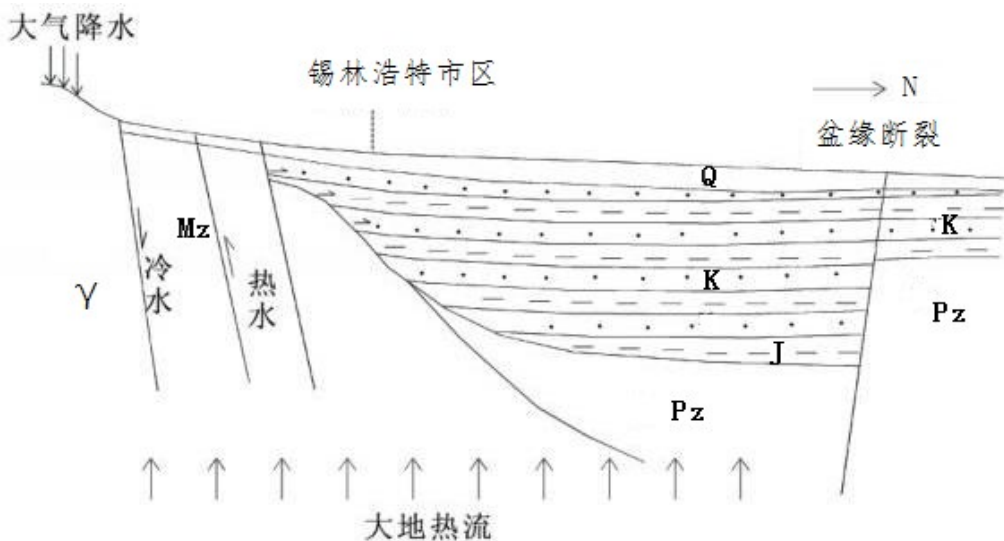


Figure 15: Sketch map of geothermal system model in the study area

Hot water temperature increase in the study area mainly relies on the deep cycle and is achieved by geothermal warming, therefore the deeper the stratus, the higher the water temperature. Studies have shown that the normal temperature of the layers is closely related to the annual average temperature and heat flow density. Therefore, we can estimate the hot water circulation depth according to the following formula:

$$Z = G (T_z - T_0) + Z_0 \quad (\text{Formula 1})$$

where: Z is the depth (m) of hot water circulation; G is geothermal depth ($\text{m}/^\circ\text{C}$), that is the reciprocal of the geothermal heating rate; T_z is the temperature (T) of the underground geothermal reservoir using the thermal storage temperature calculated by SiO_2 temperature scale; T_0 is the average temperature for many years in the recharge area, 3°C ; Z_0 is the depth of normal temperate zone, 30m.

According to data obtained by the above analysis, the calculated results for the depth of underground water circulation are shown in Table 4.

Table 4 Calculation table of depth of geothermal water circulation

Region	Geothermal gradient	Geothermal depth (G)	Thermal storage temperature (T_z)	The largest circulation depth (Z)
The north of sedimentary basin	4.4 ($^\circ\text{C}/100\text{m}$)	22.7 ($\text{m}/^\circ\text{C}$)	72 $^\circ\text{C}$	1596m
The south bedrock fissure zone	2~2.5 ($^\circ\text{C}/100\text{m}$)	40~50 ($\text{m}/^\circ\text{C}$)	55~60 $^\circ\text{C}$	2110~2880m

5. PRELIMINARY EVALUATION OF GEOTHERMAL RESOURCES

Generally, the temperature of a geothermal area increases with burial depth. However, considering the economic and technical conditions, the deeper the drilling target, the more complex the related technical requirements are, and so are the corresponding drilling costs. Therefore, the standard classifies the shallow geothermal resources above 2000 m as economical, 2000~3000 m as sub-economical, and the deeper than 3000 m as not feasible.

The Cenozoic strata of the sedimentary basin in the northern part is very thin, the thickness of the Quaternary, Tertiary and Cretaceous Bayanhua Group is about 1900 m. The sedimentary thickness of cretaceous strata is about 1600 m, the sedimentary thickness is 1400 m for the Upper Cretaceous and 200 m for the Lower Cretaceous. The main thermal reservoir in the area is mainly the Bayanhua strata of the Lower Cretaceous at a depth of 1000 m, mainly sandy gravel layers, where the temperature of heat reservoir can reach 55~60 $^\circ\text{C}$, and so belongs to the type of low temperature geothermal resources. This heat reservoir corresponds to the economical geothermal resources due to its buried depth of 1600~1800 m (the value is consistent with the hot water circulation depth value of 1596 m). The maximum depth of the hot water circulation of bedrock fissure thermal storage in the southern district is 2110~2880 m. It belongs to the middle temperature geothermal resource types due to its thermal storage temperature or up to 72 $^\circ\text{C}$.

6. CONCLUSION

The fracture thermal storage is located in a bedrock fault zone on the south of downtown, its resource quality and economic exploitation are all better than the pore type thermal storage located in Xilinhhot graben basin on the north of downtown. The priority of exploitation is suggested to be given to the former one.